



Article

# Comparing the Acidity of $(R_3P)_2BH$ -Based Donor Groups in Iridium Pincer Complexes

Leon Maser , Christian Schneider, Lukas Alig and Robert Langer \* 

Department of Chemistry, Philipps-Universität Marburg, Hans-Meerwein-Str. 4, 35032 Marburg, Germany; leon.maser@chemie.uni-marburg.de (L.M.); c.schneider2013@gmail.com (C.S.); lukas.alig@uni-goettingen.de (L.A.)

\* Correspondence: robert.langer@chemie.uni-marburg.de; Tel.: +49-6421-282-5617

Received: 31 March 2019; Accepted: 29 April 2019; Published: 7 May 2019

**Abstract:** In the current manuscript, we describe the reactivity of a series of iridium(III) pincer complexes with the general formulae  $[(PEP)IrCl(CO)(H)]^n$  ( $n = +1, +2$ ) towards base, where PEP is a pincer-type ligand with different central donor groups, and E is the ligating atom of this group ( $E = B, C, N$ ). The donor groups encompass a secondary amine, a phosphine-stabilised borylene and a protonated carbodiphosphorane. As all ligating atoms E exhibit an E–H bond, we addressed the question of whether the coordinated donor group can be deprotonated in competition to the reductive elimination of HCl from the iridium(III) centre. Based on experimental and quantum chemical investigations, it is shown that the ability for deprotonation of the coordinated ligand decreases in the order of  $(R_3P)_2CH^+ > R_2NH > (R_3P)_2BH$ . The initial product of the reductive elimination of HCl from  $[(PBP)IrCl(CO)(H)]^n$  (**1c**), the square planar iridium(I) complex,  $[(PBP)Ir(CO)]^+$  (**3c**), was found to be unstable and further reacts to  $[(PBP)Ir(CO)_2]^+$  (**5c**). Comparing the C–O stretching vibrations of the latter with those of related complexes, it is demonstrated that neutral ligands based on tricoordinate boron are very strong donors.

**Keywords:** boron; iridium; pincer; carbodiphosphorane

## 1. Introduction

Tricoordinate boron compounds,  $BR_3$ , are typically Lewis acids and stabilise their electron deficiency by  $\pi$ -donating substituents, hyperconjugation or dimerisation and formation of two-electron three-centre bonds. In consequence, they can accept electron donation from electron rich metal centres and serve as Z-type ligands [1,2]. More recently, several groups demonstrated that the introduction of  $\pi$ -accepting substituents allows to stabilise an occupied  $p_z$ -orbital and therewith of a trigonal planar Lewis-base with the general formulae  $L_2BR$  (**III**) [3–9]. Consequently, such compounds are able to serve as electron-donating or L-type ligands, but the coordination chemistry of such nucleophilic boron compounds is rather unexplored [8–10].

In particular, the similarity to related carbon compounds of the type  $L_2CH^+$  (**II**) and secondary amines (**I**) caught our attention. Pseudo-tetrahedral, secondary amines (**I**) can serve as cooperative ligands in homogeneous catalysts (Figure 1), by providing a proton in concerted proton hydride transfers or simply by pre-coordination of the substrate via hydrogen bridge bonds (e.g., in Figure 1, cycle A) [11]. Protonated carbodiphosphoranes of the type  $(R_3P)_2CH^+$  (**II**) can be deprotonated by strong bases and easily form their deprotonated analogues when coordinated to a metal centre [12]. For the corresponding boron compounds,  $(R_3P)_2BH$  (**III**), previous studies indicated that the boron-bound hydrogen atom in such ligands is not hydridic [13,14]. Due to the  $\pi$ -accepting nature of the cyanido substituents in compounds like  $[HB(CN)_3]^-$ , they can be deprotonated [15], which stands in contrast to the reactivity of the majority of hydrogen-containing boron compounds.

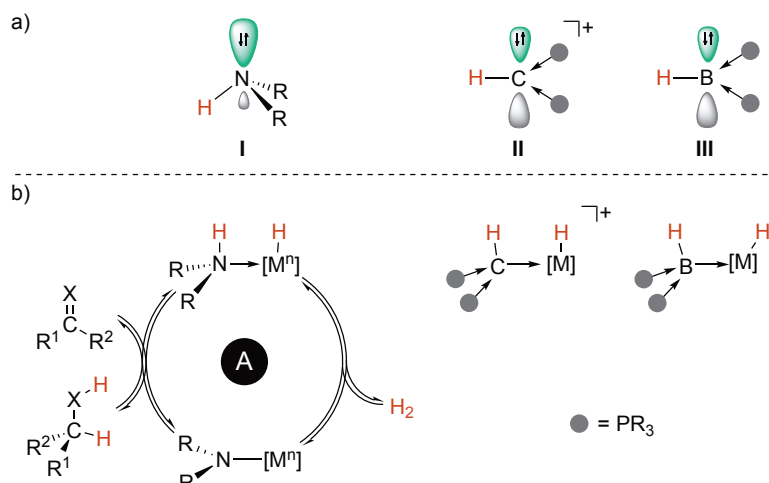


**Figure 1.** (a) Secondary amines (I), protonated carbodiphosphoranes (II) and phosphine-stabilized borylenes (III) in comparison; (b) Secondary amine ligands and their role in cooperative catalysis in comparison to the analogous metal complexes with II and III as ligands.

Motivated by these observations, we began to study a series of isotypical iridium complexes in their reactivity towards base. Herein, we demonstrate that among this series I–III the carbon-based ligand II is the most acidic ligand, while for the other ligands a competitive reductive elimination is observed. In case of the boron-based ligand, this leads to an unique iridium(I) complex. The comparison with related iridium dicarbonyl complexes reveals strong electron donating properties of donor groups akin to III.

## 2. Results and Discussion

As the starting point for our study, we choose the isotypical iridium(III) pincer complexes **1a–1c** to investigate. In this context, we compare the amine based pincer-type complex  $[\{(PPh_2CH_2CH_2)_2NH\}IrCl(CO)(H)]^+ Cl^-$  (**1a**) with the formally carbon(0)- and boron(I)-based complexes  $[\{(dppm)_2CH\}IrCl(CO)(H)]^{2+} 2 Cl^-$  (**1b**) and  $[\{(dppm)_2BH\}IrCl(CO)(H)]^+ Br^-$  (**1c**) [16]. In principle, the deprotonation of **1a–1c** can take place at several positions in the complex, but commonly either the central donor group E is deprotonated or the hydrido ligand is abstracted in a reductive elimination (Figure 2).

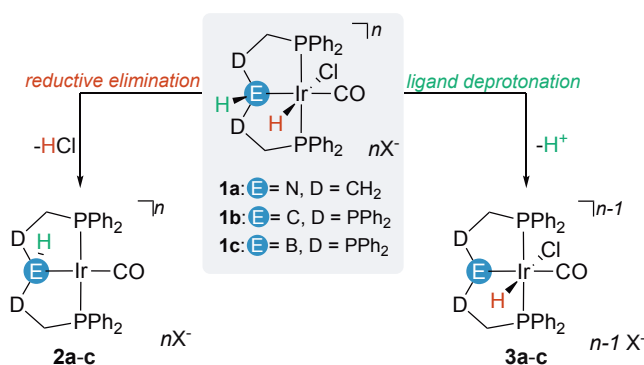


**Figure 2.** Cooperative ligand site vs. redox reactivity—principle reaction pathways of octahedral iridium(III) complexes **1a–1c** towards base ( $n = +, 2+$ ).  $X^- = Cl^-$  (a,b),  $Br^-$  (c)

### 2.1. Deprotonation vs. Reductive Elimination

The reaction of the cationic complex **1a** with one equivalent of  $LiN(SiMe_3)_2$  results in the formation of a new complex **2a** (Figure 3), as judged by the observation of a single resonance at 55.5 ppm in the  $^{31}P\{^1H\}$  NMR spectrum of the reaction mixture. The resonance at  $-16.12$  ppm in the  $^1H$  NMR spectrum,

corresponding to the hydrido ligand in **1a** disappears and the absence of a resonance in this region (0 to  $-40$  ppm) suggests that no hydrido ligand is present in the newly formed **2a** (Supplementary Materials). By comparison of NMR spectroscopic data with analogues isopropyl-substituted iridium pincer complexes [17], we concluded that the reductive elimination of HCl is the preferred reaction pathway. Addition of a second equivalent of  $\text{LiN}(\text{SiMe}_3)_2$  resulted in the formation of a mixture of complexes and the  $^{31}\text{P}\{^1\text{H}\}$  NMR spectrum displayed several new singlet resonances as well as a new AB spin system (Supplementary Materials). The latter finding either indicates a conformational change to a facially coordinated ligand with different ligands in *trans*-position, but this seems to be unlikely for a square pyramidal iridium(I) complex that is already formed with the first equivalent of base. A second possibility involves a  $\beta$ -hydride elimination from the amide ligands and subsequent tautomerisation, as previously observed for different noble metal complexes with this type of ligand [18].

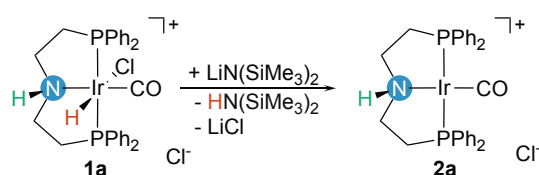


Figure 3. Reactivity of **1a** towards base.

The NMR spectra of the iridium(III) complex **1b** at ambient temperature show the presence of the *cis*- and the *trans*-isomers (ca. 1:1) as well as small quantities of **3b** (ca. 1%) [16]. The  $^1\text{H}$  NOESY NMR spectrum of **1b** at ambient temperature displays exchange correlations between the hydride resonances of *cis*- and *trans*-**1b**, as well as between the resonances of *trans*-**1b** and **3b** (Figure 4a). These findings suggest the presence of an equilibrium between the two isomers of **1b** (Figure 4b). Furthermore one of the isomers (*trans*-**1b**) seems to be in an equilibrium with the deprotonated species **1b**, even though no additional base is present in the mixture. A broad resonance at 3.51 ppm in the  $^1\text{H}$  NMR spectrum is assigned to HCl [19], which provides further support for reversible (de)protonation equilibrium. To get further insights about the solution behaviour of **1b**, we acquired  $^1\text{H}$  and  $^1\text{H}\{^{31}\text{P}\}$  NMR spectra at different temperatures. The ratio of integrals for the hydride resonances enables to estimate the equilibrium constant  $K_{cis/trans}$  at different temperatures. The corresponding *Van't Hoff* plot (Figure 4c) displays two regions of linearity between 300 and 270 K ( $R^2 = 0.995$ ) as well as between 260 and 230 K ( $R^2 = 0.937$ ), which might be related to the presence of a second equilibrium or solubility issues at low temperatures. However, a reliable quantification of **3b** turned out to be difficult, due to the low concentration at ambient temperature, which decreases even further at lower temperatures. The corresponding exchange rates were accessed by line-shape-analysis of the hydride resonances in the  $^1\text{H}\{^{31}\text{P}\}$  NMR spectra at different temperatures. An *Eyring* analysis (Figure 4d) revealed an *Gibbs* enthalpy of activation  $\Delta G_{298}^\ddagger = 69.23 \text{ kJ}\cdot\text{mol}^{-1}$  for the *cis*-/*trans*-isomerisation process.

In view of the primary question, these observations suggest that **1b** gets selectively deprotonated at the coordinated donor group. The iridium(III) complex **3b** is indeed observed by NMR spectroscopy in reactions with base. As complex **1b**, in contrast to **1a** and **1c**, is dicationic, one would expect a higher acidity of the coordinated donor group, but the acidity of hydrido ligands was previously demonstrated to be increased by several orders of magnitude with an increasing charge of the complex [20].

Addition of an excess base (DBU) to **1b** results in the formation of the iridium(I) complex **4b** as major product according to the  $^{31}\text{P}\{^1\text{H}\}$  NMR spectrum of the reaction mixture (Figure 5), which displayed new triplet resonances at 23.4 ppm ( $^2J_{\text{P,P}} = 48.5 \text{ Hz}$ ) and 38.3 ppm ( $^2J_{\text{P,P}} = 49.3 \text{ Hz}$ ). A broad multiplet resonance at 4.01–4.12 ppm with an integral of four in combination with multiplet resonances between 6.9 and 7.8 ppm with an overall integral of 40 protons are observed in the  $^1\text{H}$  NMR spectrum (Supplementary Materials), while the absence of resonances corresponding to a hydrido ligand or a protonated CDP moiety indicate that a deprotonated pincer ligand is coordinated in **4b**. The observation of one band at  $1925 \text{ cm}^{-1}$  for the C–O stretching vibration of a carbonyl ligand

is in line with an electron-rich mono-carbonyl complex. The composition of the cationic complex  $[\{(dppm)_2C\}Ir(CO)]^+ Cl^-$  in **4b** was further confirmed by high resolution ESI-MS.

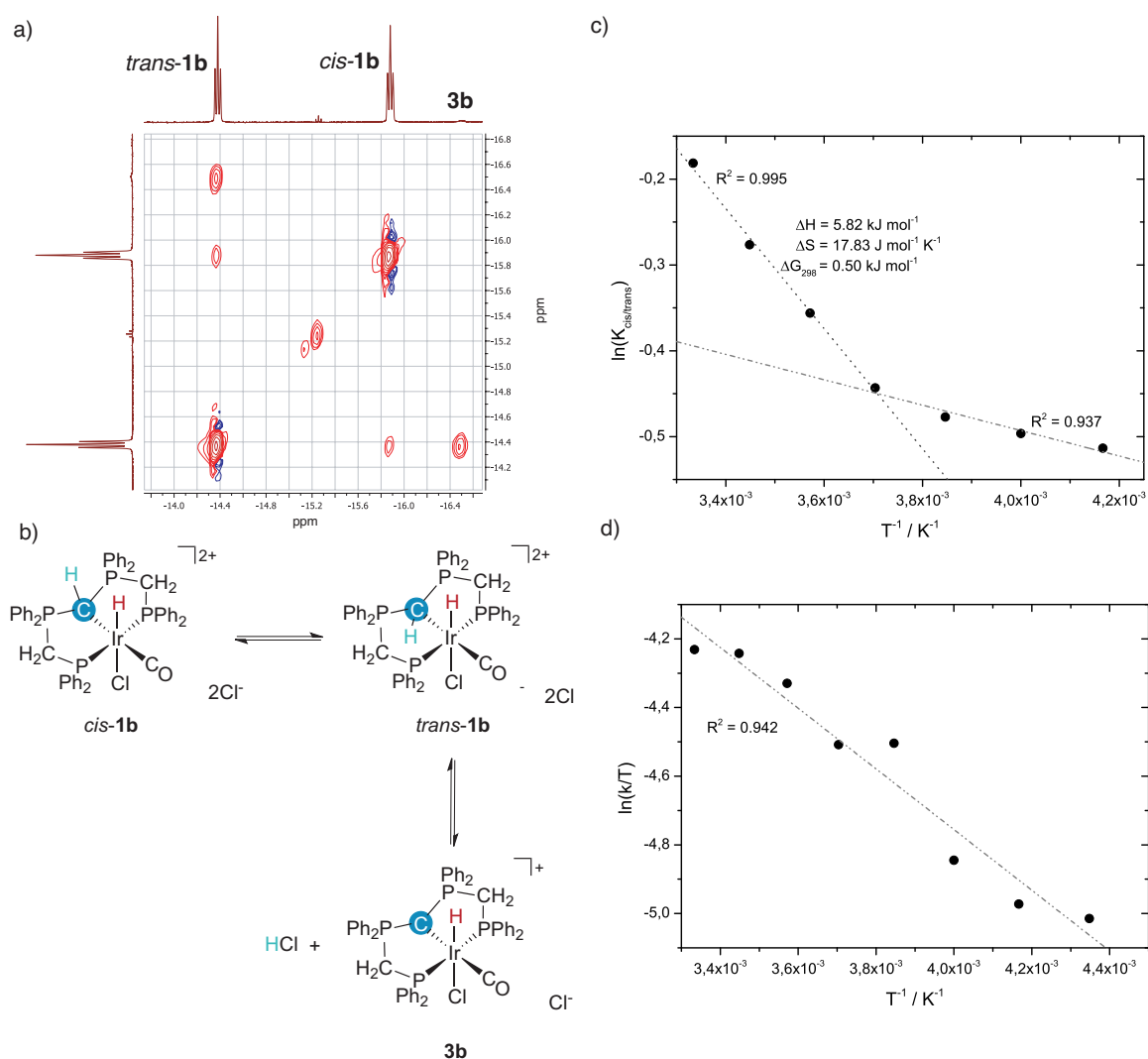


**Figure 4.** (a) Hydride region in the  $^1H$  NOESY NMR spectrum at ambient temperature, showing chemical exchange correlations; (b) Equilibrium of the complexes in solution; (c) Van't Hoff plot for the *cis*-/*trans*-isomerisation of **1b**; (d) Eyring plot for the *cis*-/*trans*-isomerisation of **1b**.

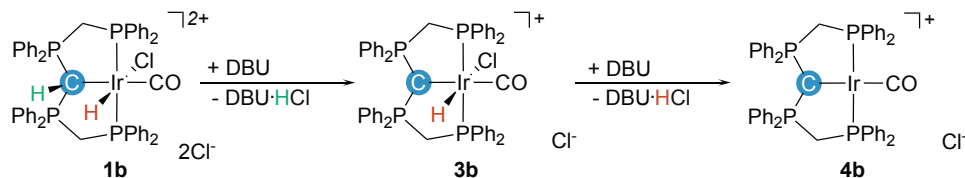


**Figure 5.** Reactivity of **1b** towards base.

A similar observation to the reaction of **1a** is made for the boron-based iridium pincer complex (**1c**). Treatment of complex **1c** with one equivalent  $LiN(SiMe_3)_2$  leads to the formation of two species according to the  $^{31}P\{^1H\}$  NMR spectrum of the reaction mixture, broadened resonance at  $-5.6$  ppm, as well as a broad resonance at  $24.9$  and a multiplet at  $2.9$  ppm, both assignable to the newly formed complex **5c** (Figure 6). After removal of all volatiles and washing of the residue with *n*-hexane, complex **5c** is obtained in analytically pure form. The  $^1H$  NMR spectrum of **5c** shows a complete set of resonances for the dppm arms of the coordinated ligand (Supplementary Materials),

while resonances corresponding to a boron-bound hydrogen atom and potential hydrido ligands are absent (Figure 7b). Upon  $^{11}\text{B}$ -decoupling a triplet resonance at 3.20 ppm ( $^2J_{\text{P,H}} = 23.2$  Hz) is observed in the  $^1\text{H}\{^{11}\text{B}\}$  NMR spectrum, assignable to a boron-bound hydrogen atom, clearly indicating that a reductive elimination is favoured over of the ligand deprotonation. The  $^{11}\text{B}\{^1\text{H}\}$  NMR spectrum of **5c** gives rise to a broadened resonance at  $-35.4$  ppm, which is in agreement with previously reported boron-based donor ligands [8–10,13,21]. The identity of **5c** was finally confirmed by single crystal X-Ray diffraction experiments (Figure 7a), which revealed a cationic iridium(I) complex with a trigonal bipyramidal environment ( $\tau_5 = 0.70$ ) [22]. In addition to the facially coordinated PBP-ligand, two carbonyl ligands are observed, one occupying an equatorial and one an axial coordination site. The Ir–B bond in **5c** is with 2.276 Å slightly shorter than in the octahedral iridium(III) complex **1c** ( $d_{\text{Ir–B}} = 2.285$  Å) [16].

As the yield of the dicarbonyl complex **5c** was below 50% and no other potential source of carbon monoxide was present in the reaction mixture, we assumed that the formation of **5c** proceeds via a square planar iridium(I) intermediate **2c** that subsequently reacts in carbonyl transfer step to **5c** and unidentified decomposition products (Figure 6). This hypothesis is further verified by an increased yield of 59% in the deprotonation reaction in the presence of carbon monoxide.

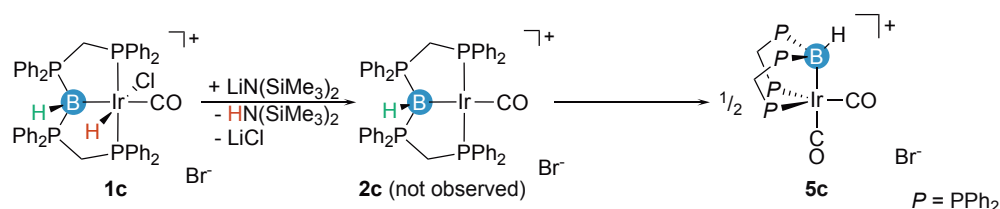


Figure 6. Reactivity of **1c** towards base.

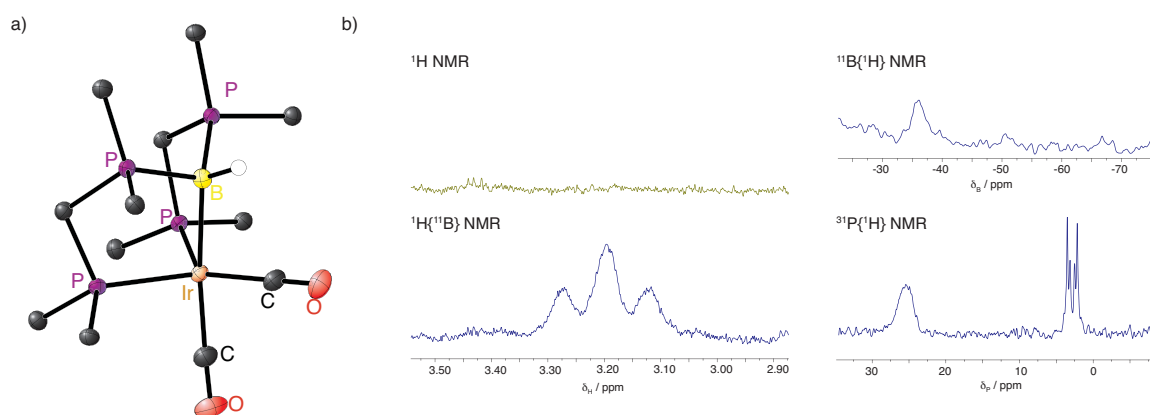


Figure 7. (a) Molecular structure of the cationic complex in **5c** in the solid state (ellipsoids are drawn at 50% probability level; carbon atoms of the phenyl rings, carbon-bound hydrogen atoms, co-crystallized solvent molecules and counter ion are omitted for clarity); (b) Selected NMR spectra of complex **5c**.

## 2.2. Proton Affinities and Deprotonation Pathways

Quantum chemical investigations using density functional theory (DFT) were performed to get further insights about the reactivity of the reported iridium complexes towards bases. First we confirmed that deprotonation of the coordinated donor group results in an energetic minimum (**3a–3c**) according to the frequency calculation (no imaginary modes) and calculated the proton affinities (PAs) for **3a–3c** (Table 1 and Figure 8). In agreement with the experimental results, complex **3b** exhibits the lowest proton affinity (PA, represents the energy difference between complexes calculated without solvation and counter ions; the energy of free proton is not considered) with  $864 \text{ kJ}\cdot\text{mol}^{-1}$ , while the PAs of the neutral complexes **3a** ( $1129 \text{ kJ}\cdot\text{mol}^{-1}$ ) and **3c** ( $1257 \text{ kJ}\cdot\text{mol}^{-1}$ ) are significantly higher.

The low PA of the CDP-group in the coordinated pincer-type ligand indicates that it might be less efficient as internal base in a potential catalyst, but in turn it suggests that protonated CDPs might be potential cooperative groups that facilitate an efficient proton-hydride-transfer from or to the catalyst.

In comparison, the value of  $1257 \text{ kJ}\cdot\text{mol}^{-1}$  is too high to expect metal-ligand-cooperativity via proton-hydride-transfer, but it clearly suggests that deprotonation of coordinated  $(\text{R}_3\text{P})_2\text{BH}$  groups should be facile with strong bases in the absence of more acidic sites, which would yield an unprecedented phosphine-stabilized boride.

**Table 1.** Calculated Proton affinities of complexes **3a–3c** and **6a–6c** (G16, B97D/def2-TZVPP).

Donor in <b>1</b>	Reactivity	PA(3)/ $\text{kJ}\cdot\text{mol}^{-1}$	Reactivity	PA(6)/ $\text{kJ}\cdot\text{mol}^{-1}$	$\Delta\text{PA}/\text{kJ}\cdot\text{mol}^{-1}$
$\text{R}_2\text{NH}$	<b>1a</b> → <b>3a</b>	1129	<b>1a</b> → <b>6a</b>	1126	3
$(\text{Ph}_2\text{RP})_2\text{CH}$	<b>1b</b> → <b>3b</b>	864	<b>1b</b> → <b>6b</b>	900	−36
$(\text{Ph}_2\text{RP})_2\text{BH}$	<b>1c</b> → <b>3c</b>	1257	<b>1c</b> → <b>6c</b>	1175	82

To elucidate the reductive elimination pathway, we removed a proton from the metal-coordinated hydrido ligand in **1a–1c** in a *gedankenexperiment* and performed geometry optimisations. The resulting complexes (**6a–6c**) exhibit elongated iridium chloride distances (Figure 8), but were confirmed as energetic minima by frequency calculations. Although the Ir–Cl distances in **6a–6c** are in range between a weak bond ( $2.737 \text{ \AA}$ ) and non-bonding ( $4.181 \text{ \AA}$ ), the resulting proton affinities may be used as estimate in comparison to **3a–3c**.

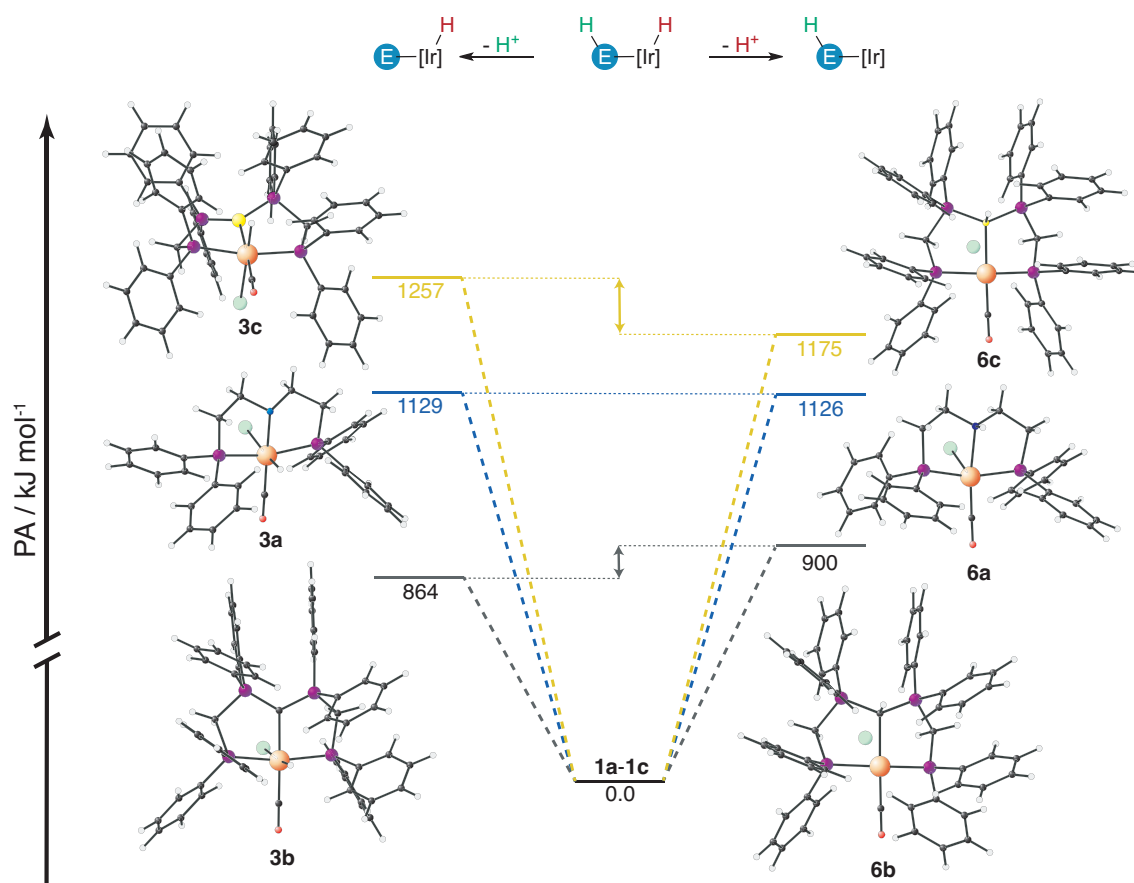


**Figure 8.** Proton affinities and DFT-optimized structures of **3a–3c** and **6a–6c** (G16, B97D/def2-TZVPP).

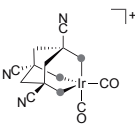
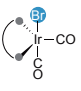
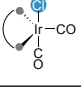
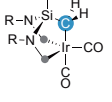
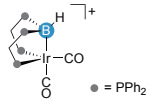
It becomes evident that in case of the amine-based ligand product of ligand- (**3a**) and metal-deprotonation (**6a**) exhibit very similar proton affinities ( $\Delta\text{PA} = 3 \text{ kJ}\cdot\text{mol}^{-1}$ ), which suggests that

both pathways are in principle favourable. The experimentally observed selectivity for the reductive elimination might be kinetically favoured. In case of the protonated CDP-based ligand in **1b** the ligand deprotonation is favoured  $36 \text{ kJ}\cdot\text{mol}^{-1}$  over the deprotonation at the metal site, which again is in line with the experimental observations. Notably, both PAs, of **3b** and **6b**, are rather low. For the boron-based pincer-type ligand in **1c** the deprotonation at the metal centre is clearly favoured.

### 2.3. Comparison with Related Iridium(I) Dicarbonyl Complexes

In comparison to related trigonal bipyramidal iridium(I) dicarbonyl complexes, **5c** exhibits very similar structural features (Table 2). All complexes with two  $\text{Ph}_2\text{RP}$ -groups and one carbonyl ligand in the equatorial plane differ in the ligand or donor group in the apical position, *trans* to the second carbonyl ligand [23–25]. With  $\tau_5$ -parameters between 0.58 and 0.75, four of the five complexes are best described as trigonal bipyramidal complexes. In the IR spectrum, two bands for the C–O-stretching frequency are observed for each complex, which in principle allow to estimate the net electron donor ability of the specified donor group in comparison. Like for other dicarbonyl-based ligand parameters [26–28], averaging of *cis*- and *trans*-influences on symmetric and asymmetric C–O-stretching modes can provide a rough picture of the net donor strength. For the neutral complexes, all values, respectively, indicate an increasing donor ability in the order  $\text{R}_3\text{SiCH}_2^- > \text{Cl}^- > \text{Br}^-$ . The cationic complex with a  $\text{Ph}_2\text{RP}$ -group in the apical position gives rise to an increased value of  $\tilde{\nu}_{\text{CO}}(\text{av}) = 1996 \text{ cm}^{-1}$ , confirming that anionic ligands exhibit stronger donor abilities. An unexpected finding in this context is the low value measured for complex **5c** ( $\tilde{\nu}_{\text{CO}}(\text{av}) = 1958 \text{ cm}^{-1}$ ), which is significantly lower than those of the anionic donor groups. Despite the fact that donor groups based on  $(\text{Ph}_3\text{P})_2\text{BH}$  are overall neutral, this observation suggests that they are stronger donors than alkyl-ligands, which are known as one of the strongest donors in coordination and organometallic chemistry.

**Table 2.** Comparison of Iridium(I) dicarbonyl complexes from literature with the new complex **5c**.

Complex	Donor	$\tau_5$	$\tilde{\nu}_{\text{CO}}/\text{cm}^{-1}$	$\tilde{\nu}_{\text{CO}}(\text{av})/\text{cm}^{-1}$	Ref.
	$\text{Ph}_2\text{RP}$	0.42	2047, 1944	1996	[23]
	$\text{Br}^-$	0.70	2023, 1950	1987	[24]
	$\text{Cl}^-$	0.58	2017, 1944	1981	[24]
	$\text{R}_3\text{SiCH}_2^-$	0.75	2001, 1927	1964	[25]
	$(\text{R}_3\text{P})_2\text{BH}$	0.70	2000, 1916	1958	this work

### 3. Materials and Methods

All experiments were carried out under an atmosphere of purified argon or nitrogen in the MBraun glove boxes LABmaster 130 and UNILab or using standard Schlenk techniques. THF and diethyl ether were dried over Na/K alloy, n-hexane was dried over  $\text{LiAlH}_4$ , toluene was dried over

sodium, dichloromethane was dried over  $\text{CaH}_2$ , methanol was dried over magnesium and ethyl acetate was dried over potassium carbonate. After drying, solvents were stored over appropriate molecular sieves. Deuterated solvents were degassed with freeze-pump-thaw cycles and stored over appropriate molecular sieves under argon atmosphere. Complexes **1a–1c** synthesised according to previously reported procedures [16].

$^1\text{H}$ ,  $^{13}\text{C}$ ,  $^{11}\text{B}$  and  $^{31}\text{P}$  NMR spectra were recorded using Bruker BioSpin GmbH (Rheinstetten, Germany) Avance HD 250, 300 A, DRX 400, DRX 500 and Avance 500 NMR spectrometers at 300 K.  $^1\text{H}$  and  $^{13}\text{C}\{^1\text{H}\}$ ,  $^{13}\text{C}$ -APT (attached proton test) NMR chemical shifts are reported in ppm downfield from tetramethylsilane. The resonance of the residual protons in the deuterated solvent was used as internal standard for  $^1\text{H}$  NMR spectra. The solvent peak of the deuterated solvent was used as internal standard for  $^{13}\text{C}$  NMR spectra. The assignment of resonances in  $^1\text{H}$  and  $^{13}\text{C}$  NMR spectra was further supported by  $^1\text{H}$  COSY,  $^1\text{H}$  NOESY,  $^1\text{H}$ ,  $^{13}\text{C}$  HMQC and  $^1\text{H}$ ,  $^{13}\text{C}$  HMBC NMR spectra.  $^{11}\text{B}$  NMR chemical shifts are reported in ppm downfield from  $\text{BF}_3 \cdot \text{Et}_2\text{O}$  and referenced to an external solution of  $\text{BF}_3 \cdot \text{Et}_2\text{O}$  in  $\text{CDCl}_3$ .  $^{31}\text{P}$  NMR chemical shifts are reported in ppm downfield from  $\text{H}_3\text{PO}_4$  and referenced to an external 85 % solution of phosphoric acid in  $\text{D}_2\text{O}$ . The following abbreviations are used for the description of NMR data: br (broad), s (singlet), d (doublet), t (triplet), q (quartet), quin (quintet), m (multiplet). FT-IR spectra were recorded by attenuated total reflection of the solid samples on a Bruker Tensor IF37 spectrometer. The intensity of the absorption band is indicated as w (weak), m (medium), s (strong), vs (very strong) and br (broad). HR-ESI mass spectra were acquired with a LTQ-FT mass spectrometer (Thermo Fisher Scientific, Waltham, MA, USA). The resolution was set to 100,000.

**Reactivity of  $[(\{\text{Ph}_2\text{PCH}_2\text{CH}_2\}_2\text{NH})\text{IrCl}(\text{CO})(\text{H})]\text{Cl}$  (**1a**) towards base** 20 mg  $[(\{\text{Ph}_2\text{PCH}_2\text{CH}_2\}_2\text{NH})\text{IrCl}(\text{CO})(\text{H})]\text{Cl}$  (**1a**, 27.3  $\mu\text{mol}$ , 1.0 eq.) and 4.6 mg LiHMDS (27.5  $\mu\text{mol}$ , 1.0 eq.) were suspended in 0.6 mL THF- $d_8$ . After stirring for 16 h, the resulting light orange suspension was filtered and, after addition of 0.2 mL THF- $d_8$ , the first NMR spectra were recorded.  $[(\{\text{Ph}_2\text{PCH}_2\text{CH}_2\}_2\text{NH})\text{Ir}(\text{CO})]\text{Cl}$  (**2a**) was identified as the main product, while small amounts of **1a** remained unreacted. Further 4.7 mg of LiHMDS (27.5  $\mu\text{mol}$ , 1.0 eq.) were added, upon which the color changed to a dark orange, and the second set of NMR spectra were recorded.

NMR spectra after addition of 1.0 eq. LiHMDS:  $^1\text{H}$  NMR (300 MHz, THF- $d_8$ , 300 K):  $\delta = 2.61\text{--}2.86$  (m, 4H,  $\text{CH}_2$ ), 3.08–3.46 (m, 4H,  $\text{CH}_2$ ), 7.03–7.24 (m, 4H,  $\text{H}_{\text{arom}}$ ), 7.25–7.51 (m, 12H,  $\text{H}_{\text{arom}}$ ), 7.73–8.03 (m, 4H,  $\text{H}_{\text{arom}}$ ) ppm. Neither N–H nor Ir–H resonances could be identified.  $^{31}\text{P}\{^1\text{H}\}$  NMR (122 MHz, THF- $d_8$ , 300 K)  $\delta = 31.7$  (s, **1a**), 55.5 (br s, **2a**) ppm.

NMR spectra after addition of 2.0 eq. LiHMDS:  $^{31}\text{P}\{^1\text{H}\}$  NMR (122 MHz, THF- $d_8$ , 300 K)  $\delta = -3.8$  (s),  $-0.9$  (s), 25.0 (s), 31.9 (s, **1a**), 36.1 (s), 39.8 (d,  $J_{\text{PP}} = 291.7$  Hz), 52.6 (d,  $J_{\text{PP}} = 292.3$  Hz), 56.1 (br s, **2a**) ppm.  $^1\text{H}$  NMR (300 MHz, THF- $d_8$ , 300 K): Due to the multiple decomposition products visible in the  $^{31}\text{P}\{^1\text{H}\}$  NMR spectrum, no analysis was performed.

**Formation of  $[(\{\text{dppm}\}_2\text{C})\text{Ir}(\text{CO})]\text{Cl}$  (**4b**)** 57 mg  $[(\{\text{dppm}\}_2\text{CH})\text{IrCl}(\text{CO})(\text{H})]\text{Cl}_2$  (**1b**, 51.4  $\mu\text{mol}$ , 1.0 eq.) were dissolved in 2 mL deuterated dichloromethane. After addition of 15.3  $\mu\text{L}$  DBU (103  $\mu\text{mol}$ , 2.0 eq.), the solution changed color from colorless to yellow. After removal of the solvent in vacuo, a yellow solid remained, containing  $[(\{\text{dppm}\}_2\text{C})\text{Ir}(\text{CO})]\text{Cl}$  (**4b**).  $^1\text{H}$  NMR (300 MHz,  $\text{CD}_2\text{Cl}_2$ , 300 K):  $\delta = 4.01\text{--}4.12$  (m, 4H,  $\text{CH}_2$ ), 7.06–7.18 (m, 8H,  $\text{H}_{\text{arom}}$ ), 7.25–7.46 (m, 24H,  $\text{H}_{\text{arom}}$ ), 7.59–7.78 (m, 8H,  $\text{H}_{\text{arom}}$ ) ppm.  $^{13}\text{C}$  APT NMR (75 MHz,  $\text{CD}_2\text{Cl}_2$ , 300 K):  $\delta = 129.0\text{--}129.3$  (m,  $\text{C}_{\text{arom}}$ ), 131.4 (br s,  $\text{C}_{\text{arom}}$ ), 132.7 (br s,  $\text{C}_{\text{arom}}$ ), 132.9 (t,  $J_{\text{C,P}} = 5.1$  Hz,  $\text{C}_{\text{arom}}$ ), 133.4 (t,  $J_{\text{C,P}} = 7.2$  Hz,  $\text{C}_{\text{arom}}$ ) ppm. Neither the carbonyl nor the  $\text{CH}_2$  resonances were observed.  $^{31}\text{P}\{^1\text{H}\}$  NMR (122 MHz,  $\text{CD}_2\text{Cl}_2$ , 300 K)  $\delta = 23.4$  (t,  $^2J_{\text{PP}} = 48.5$  Hz), 38.3 (t,  $^2J_{\text{PP}} = 49.3$  Hz) ppm. FT-IR/ $\text{cm}^{-1}$ : 3050 (w), 2962 (w), 2932 (m), 2925 (m), 2858 (m), 2855 (w), 2013 (w), 1979 (w), 1925 (s, CO), 1646 (s), 1612 (s), 1586 (s), 1481 (m), 1434 (s), 1323 (s), 1207 (w), 1119 (m), 1103 (m), 1097 (s), 1070 (s), 824 (m), 740 (s), 721 (m), 691 (s), 543 (m), 527 (m), 503 (s), 481 (s). HRMS: (ESI+, MeCN/ $\text{CH}_2\text{Cl}_2$ ): 1001.1966  $[(\{\text{dppm}\}_2\text{C})\text{Ir}(\text{CO})]^+$  measured, 1001.1972 calculated,  $\Delta = 0.60$  ppm.



**Synthesis of  $[(\text{dppm})_2\text{BH}]\text{Ir}(\text{CO})_2\text{Br}$  (5c)** Complex **1c** was generated in situ by the reaction of 90.0 mg  $[\text{IrCl}(\text{CO})(\text{PPh}_3)_2]$  (116  $\mu\text{mol}$ ) with 100.0 mg of  $[(\text{dppm})_2\text{BH}_2]\text{Br}$  (116  $\mu\text{mol}$ , 1.0 eq.) in 5 mL THF. The resulting solution of **1c** was cooled to  $-74^\circ\text{C}$  and 20.0 mg  $\text{LiN}(\text{SiMe}_3)_2$  (116  $\mu\text{mol}$ , 1.0 eq.) dissolved in 2 mL THF were added drop-wise. The reaction mixture was allowed to warm to ambient temperature, the argon atmosphere was replaced by carbon monoxide and the mixture was stirred for further two hours at ambient temperature. All volatiles were removed in vacuo, the residue was washed with 5 mL toluene and dried under high vacuum to yield 74.0 mg of a colorless solid, containing  $[(\text{dppm})_2\text{BH}]\text{Ir}(\text{CO})_2\text{Br}$  (**4c**, 68  $\mu\text{mol}$ , 59 %).  $^{31}\text{P}\{^1\text{H}\}$  NMR (101.3 MHz,  $\text{CD}_2\text{Cl}_2$ , 300 K):  $\delta = 25.4$  (br, 2P, P–B–P), 3.5–2.2 (m, 2P, P–Ir–P) ppm.  $^{11}\text{B}\{^1\text{H}\}$  NMR (96.3 MHz,  $\text{CD}_2\text{Cl}_2$ , 300 K):  $\delta = -35.4$  (br, 1B, BH) ppm. Only resonances that are change upon  $^{11}\text{B}$ -decoupling are reported in the  $^1\text{H}\{^{11}\text{B}\}$  NMR spectrum.  $^1\text{H}$  NMR (300 MHz,  $\text{CD}_2\text{Cl}_2$ , 300 K):  $\delta = 7.51\text{--}7.66$  (m, 4H,  $H_{\text{arom.}}$ ), 7.40–7.49 (m, 8H,  $H_{\text{arom.}}$ ), 7.08–7.31 (m, 8H,  $H_{\text{arom.}}$ ), 6.82–7.10 (m, 20H,  $H_{\text{arom.}}$ ), 5.42–5.61 (m, 2H,  $\text{CH}_2$ ), 4.07–4.16 (m, 2H,  $\text{CH}_2$ ) ppm.  $^1\text{H}\{^{11}\text{B}\}$  NMR (300 MHz,  $\text{CD}_2\text{Cl}_2$ , 300 K)  $\delta = 3.20$  (t,  $^2 J_{\text{HP}} = 23.2$  Hz, 1H, BH) ppm.  $^{13}\text{C}\{^1\text{H}\}$  NMR (121.5 MHz,  $\text{CD}_2\text{Cl}_2$ , 300 K)  $\delta = 134.7$  (vt, 4C,  $C_{\text{arom.}}$ ), 133.5 (s, 4C,  $C_{\text{arom.}}$ ), 133.0 (s, 4C,  $C_{\text{arom.}}$ ), 132.0 (s, 4C,  $C_{\text{arom.}}$ ), 131.3 (s, 4C,  $C_{\text{arom.}}$ ), 130.9 (vt, 4C,  $C_{\text{arom.}}$ ), 130.2 (s, 4C,  $C_{\text{arom.}}$ ), 129.2 (s, 4C,  $C_{\text{arom.}}$ ), 129.2 (s, 4C,  $C_{\text{arom.}}$ ), 128.9 (s, 4C,  $C_{\text{arom.}}$ ), 128.7 (s, 4C,  $C_{\text{arom.}}$ ), 128.3 (s, 4C,  $C_{\text{arom.}}$ ), 33.5 (vt, 1C,  $\text{CH}_2$ ), 30.3 (vt, 1C,  $\text{CH}_2$ ) ppm. FT-IR:  $\tilde{\nu}/\text{cm}^{-1} = 3050$  (w), 3017 (w), 2962 (w), 2823 (w), 2724 (w), 2000 (s, CO), 1916 (s, CO), 1586 (w), 1574 (w), 1483 (m), 1434 (s), 1379 (w), 1333 (w), 1306 (w), 1260 (m), 1094 (s), 1024 (s), 869 (w), 797 (s), 778 (s), 731 (vs), 685 (vs), 616 (w), 554 (m), 523 (s), 480 (s). HRMS (ESI+, MeOH)  $m/z = 969.1884$   $[(\text{dppm})_2\text{BH}]\text{Ir}(\text{CO})_2^+$ , calc. 969.1887 ( $\Delta = 0.31$  ppm).

#### 4. Conclusions

In the current manuscript, we reported the first iridium(I) complex formally containing phosphine-stabilised borylene as a donor group. The comparison to related iridium(I) dicarbonyl complexes suggests strong donor properties of this type of nucleophilic boron compounds. In an internal competition with a hydrido-ligand, the reactivity towards base reveals that analogous carbon compounds and protonated CDPs are easy to deprotonate, while only strong bases contribute to deprotonate phosphine-stabilized borylenes in the coordination sphere of a central metal atom.

**Supplementary Materials:** The following are available online at <http://www.mdpi.com/2304-6740/7/5/61/s1>, Figures S1–S12: NMR and IR spectra of compounds **2a**, **4b** and **5c**; Table S1: crystallographic data for compound **5c**; xyz-coordinates.

**Author Contributions:** L.M., C.S. and L.A. performed the experiments. All calculations were made by L.M., R.L. and L.M. wrote the manuscript. R.L. designed and directed the project.

**Funding:** This work was supported by the Deutsche Forschungsgemeinschaft (LA 2830/3-2, 2830/5-1 and 2830/6-1).

**Acknowledgments:** R.L. is grateful to S. Dehnen for her continuous support.

**Conflicts of Interest:** The authors declare no conflict of interest.

#### Abbreviations

The following abbreviations are used in this manuscript:

CDP	carbodiphosphorane
DBU	1,8-Diazabicyclo[5.4.0]undec-7-ene
dppm	1,1-bis(diphenylphosphino)methane
DFT	density functional theory
ESI	electro spray ionisation
HMDS	hexamethyldisilazane
NMR	nuclear magnetic resonance
HRMS	high resolution mass spectrometry
THF	tetrahydrofuran

## References

1. Bouhadir, G.; Bourissou, D. Complexes of ambiphilic ligands: reactivity and catalytic applications. *Chem. Soc. Rev.* **2016**, *45*, 1065–1079. [[CrossRef](#)]
2. Amgoune, A.; Bourissou, D.  $\sigma$ -Acceptor, Z-type ligands for transition metals. *Chem. Commun.* **2011**, *47*, 859–871. [[CrossRef](#)]
3. Braunschweig, H.; Dewhurst, R.D.; Hupp, F.; Nutz, M.; Radacki, K.; Tate, C.W.; Vargas, A.; Ye, Q. Multiple complexation of CO and related ligands to a main-group element. *Nature* **2015**, *522*, 327–330. [[CrossRef](#)]
4. Landmann, J.; Sprenger, J.A.P.; Bertermann, R.; Ignat'ev, N.; Bernhardt-Pitchougina, V.; Bernhardt, E.; Willner, H.; Finze, M. Convenient access to the tricyanoborate dianion  $B(CN)_3^{2-}$  and selected reactions as a boron-centred nucleophile. *Chem. Commun.* **2015**, *51*, 4989–4992. [[CrossRef](#)]
5. Bernhardt, E.; Bernhardt-Pitchougina, V.; Willner, H.; Ignatiev, N. "Umpolung" at boron by reduction of  $[B(CN)_4]^-$  and formation of the dianion  $[B(CN)_3]^{2-}$ . *Angew. Chem. Int. Ed.* **2011**, *50*, 12085–12088. [[CrossRef](#)]
6. Kinjo, R.; Donnadiou, B.; Celik, M.A.; Frenking, G.; Bertrand, G. Synthesis and characterization of a neutral tricoordinate organoboron isoelectronic with amines. *Science* **2011**, *333*, 610–613. [[CrossRef](#)]
7. Ruiz, D.A.; Melaimi, M.; Bertrand, G. An efficient synthetic route to stable bis(carbene)borylenes  $[(L_1)(L_2)BH]$ . *Chem. Commun.* **2014**, *50*, 7837–7839. [[CrossRef](#)]
8. Kong, L.; Li, Y.; Ganguly, R.; Vidovic, D.; Kinjo, R. Isolation of a Bis(oxazol-2-ylidene)-phenylborylene adduct and its reactivity as a boron-centered nucleophile. *Angew. Chem. Int. Ed.* **2014**, *53*, 9280–9283. [[CrossRef](#)]
9. Kong, L.; Ganguly, R.; Li, Y.; Kinjo, R. Diverse reactivity of a tricoordinate organoboron  $L_2PhB$ : (L = oxazol-2-ylidene) towards alkali metal, group 9 metal, and coinage metal precursors. *Chem. Sci.* **2015**, *6*, 2893–2902. [[CrossRef](#)]
10. Ruiz, D.A.; Ung, G.; Melaimi, M.; Bertrand, G. Deprotonation of a Borohydride: Synthesis of a Carbene-Stabilized Boryl Anion. *Angew. Chem. Int. Ed.* **2013**, *52*, 7590–7592. [[CrossRef](#)]
11. Dub, P.A.; Gordon, J.C. The mechanism of enantioselective ketone reduction with Noyori and Noyori–Ikariya bifunctional catalysts. *Dalton Trans.* **2016**, *45*, 6756–6781. [[CrossRef](#)]
12. Maser, L.; Herritsch, J.; Langer, R. Carbodiphosphorane-based nickel pincer complexes and their (de)protonated analogues: Dimerisation, ligand tautomers and proton affinities. *Dalton Trans.* **2018**, *47*, 10544–10552. [[CrossRef](#)]
13. Vondung, L.; Frank, N.; Fritz, M.; Alig, L.; Langer, R. Phosphine-Stabilized Borylenes and Boryl Anions as Ligands? Redox Reactivity in Boron-Based Pincer Complexes. *Angew. Chem. Int. Ed.* **2016**, *55*, 14450–14454. [[CrossRef](#)]
14. Vondung, L.; Jerabek, P.; Langer, R. Ligands Based on Phosphine-Stabilized Aluminum(I), Boron(I), and Carbon(0). *Chem. Eur. J.* **2019**, *25*, 3068–3076. [[CrossRef](#)]
15. Landmann, J.; Keppner, F.; Hofmann, D.B.; Sprenger, J.A.; Höring, M.; Zotnick, S.H.; Müller-Buschbaum, K.; Ignat'ev, N.V.; Finze, M. Deprotonation of a Hydridoborate Anion. *Angew. Chem. Int. Ed.* **2017**, *56*, 2795–2799. [[CrossRef](#)]
16. Maser, L.; Schneider, C.; Vondung, L.; Alig, L.; Langer, R. Quantifying the Donor Strength of Ligand-Stabilized Main Group Fragments. *J. Am. Chem. Soc.* **2019**. [[CrossRef](#)]
17. Friedrich, A.; Ghosh, R.; Kolb, R.; Herdtweck, E.; Schneider, S. Iridium olefin complexes bearing dialkylamino/amido PNP pincer ligands: Synthesis, reactivity, and solution dynamics. *Organometallics* **2009**, *28*, 708–718. [[CrossRef](#)]
18. Schneider, S.; Meiners, J.; Askevold, B. Cooperative aliphatic PNP amido pincer ligands-versatile building blocks for coordination chemistry and catalysis. *Eur. J. Inorg. Chem.* **2012**, *2012*, 412–429. [[CrossRef](#)]
19. Cheng, F.; Yang, X.; Peng, H.; Chen, D.; Jiang, M. Well-controlled formation of polymeric micelles with a nanosized aqueous core and their applications as nanoreactors. *Macromolecules* **2007**, *40*, 8007–8014. [[CrossRef](#)]
20. Morris, R.H. Estimating the acidity of transition metal hydride and dihydrogen complexes by adding ligand acidity constants. *J. Am. Chem. Soc.* **2014**, *136*, 1948–1959. [[CrossRef](#)]
21. Grätz, M.; Bäcker, A.; Vondung, L.; Maser, L.; Reincke, A.; Langer, R. Donor ligands based on tricoordinate boron formed by B–H-activation of bis(phosphine)boronium salts. *Chem. Commun.* **2017**, *53*, 7230–7233. [[CrossRef](#)]

22. Addison, A.W.; Rao, T.N.; Reedijk, J.; van Rijn, J.; Verschoor, G.C.; Trans, D.; Addison, A.W.; Rao, T.N. Synthesis, structure, and spectroscopic properties of copper(II) compounds containing nitrogen–sulphur donor ligands; the crystal and molecular structure of aqua[1,7-bis(*N*-methylbenzimidazol-2'-yl)-2,6-dithiaheptane]copper(II) perchlorate. *Dalton Trans. J. Chem. Soc.* **1984**, 1349–1356. [[CrossRef](#)]
23. Heins, W.; Mayer, H.A.; Fawzi, R.; Steimann, M. Stereochemical and Electronic Control of Functionalized Tripodal Phosphines. Reactivity of the Adamantane-Type Ir(tripod)(CO)Cl (tripod = *cis,cis*-1,3,5-(PPh<sub>2</sub>)<sub>3</sub>-1,3,5-X<sub>3</sub>C<sub>6</sub>H<sub>6</sub>; X = H, COOMe, CN) Complexes toward H<sup>+</sup>, H<sub>2</sub>, CO, and C<sub>2</sub>H<sub>4</sub>. *Organometallics* **1996**, *15*, 3393–3403. [[CrossRef](#)]
24. Fox, D.J.; Duckett, S.B.; Flaschenriem, C.; Brennessel, W.W.; Schneider, J.; Gunay, A.; Eisenberg, R. A Model Iridium Hydroformylation System with the Large Bite Angle Ligand Xantphos: Reactivity with Parahydrogen and Implications for Hydroformylation Catalysis. *Inorg. Chem.* **2006**, *45*, 7197–7209. [[CrossRef](#)]
25. Passarelli, V.; Pérez-Torrente, J.J.; Oro, L.A. Intramolecular C–H Oxidative Addition to Iridium(I) in Complexes Containing a *N,N'*-Diphosphanosilanediamine Ligand. *Inorg. Chem.* **2014**, *53*, 972–980. [[CrossRef](#)]
26. Chianese, A.R.; Li, X.; Janzen, M.C.; Faller, J.W.; Crabtree, R.H. Rhodium and iridium complexes of *N*-heterocyclic carbenes via transmetalation: Structure and dynamics. *Organometallics* **2003**, *22*, 1663–1667. [[CrossRef](#)]
27. Kelly III, R.A.; Clavier, H.; Giudice, S.; Scott, N.M.; Stevens, E.D.; Bordner, J.; Samardjiev, I.; Hoff, C.D.; Cavallo, L.; Nolan, S.P. Determination of *N*-Heterocyclic Carbene (NHC) Steric and Electronic Parameters using the [(NHC)Ir(CO)<sub>2</sub>Cl] System. *Organometallics* **2008**, *27*, 202–210. [[CrossRef](#)]
28. Wolf, S.; Plenio, H. Synthesis of (NHC)Rh(cod)Cl and (NHC)RhCl(CO)<sub>2</sub> complexes—Translation of the Rh into the Ir-scale for the electronic properties of NHC ligands. *J. Organomet. Chem.* **2009**, *694*, 1487–1492. [[CrossRef](#)]



© 2019 by the authors. Licensee MDPI, Basel, Switzerland. This article is an open access article distributed under the terms and conditions of the Creative Commons Attribution (CC BY) license (<http://creativecommons.org/licenses/by/4.0/>).